Computerized Simulation of Automotive Air-Conditioning System: Development of Mathematical Model and Its Validation

Haslinda Mohamed Kamar[1], Mohd Yusoff Senawi[2] and Nazri Kamsah[3]

[1] Department of Thermo-Fluid, Universiti Teknologi Malaysia
81310 UTM Skudai, Johor, Malaysia

[2] Department of Thermo-Fluid, Universiti Teknologi Malaysia
81310 UTM Skudai, Johor, Malaysia

[3] Department of Thermo-Fluid, Universiti Teknologi Malaysia
81310 UTM Skudai, Johor, Malaysia

Abstract

A semi-empirical model for simulating thermal and energy performance of an automotive air-conditioning (AAC) system in passenger vehicles has been developed. The model consists of two sections, namely empirical evaporator correlations and dynamic load simulation. The correlations used consider sensible and latent heat transfer performance of the evaporator coil. The correlations were obtained from the experimental data of actual air conditioning system for a compact size passenger car. The sensible heat transfer correlation relates the evaporator air off dry-bulb temperature to inlet air dry-bulb temperature, humidity ratio, evaporator air velocity, condenser inlet air dry-bulb temperature, condenser air velocity and compressor speed. The latent heat transfer correlation relates the coil air-off humidity ratio to the same six independent variables. The dynamic load simulation model was developed based on the z-transfer function method with a one-minute time step. The cooling load calculations were performed using heat gain weighting factors. Heat extraction rate and cabin air dry-bulb temperature calculations were carried out using air temperature weighting factors. The empirical evaporator sensible and latent heat transfer correlations were embedded in the loads calculation program to enable the determination of evaporator inlet and outlet air conditions, the cabin air temperature and relative humidity. Comparisons with road test data indicated that the program was capable of predicting the performance of the automotive air-conditioning system with reasonable accuracy.

Keywords: *Automotive air conditioning (AAC), passenger cabin, thermal load model.*

1. Introduction

Automotive air-conditioning (AAC) for thermal comfort in passenger cabins is now a thing of necessity rather than luxury, and cooling is especially needed when travelling in summer or throughout the year in countries of hot and humid climate. The cost of installation of this air-conditioning system is generally affordable but the extra weight added and the system operation both cause the fuel consumption to increase. Additional fuel consumption by the AAC system means less fuel economy and more greenhouse gas emissions. Consequently, augmentation of the AAC efficiency and evaluation of its performance are both important. The AAC is often exposed to extremely varying conditions, and substantial efforts are required to evaluate its performance. The conditions include: inlet conditions which determine air temperatures entering the evaporator and condenser; user choices which determine the evaporator volumetric flow rate and ventilation mode; driving patterns which determine the compressor rotational speed and the condenser face velocity; and cabin material, occupancy, and weather conditions which determine internal and external thermal loads [1].

The single largest auxiliary load on an automotive engine is caused by the air-conditioner compressor [2]. During peak load it can draw up to 5 to 6 kW power from the vehicle's engine, and this is equivalent to a vehicle being driven down the road at 56 km/hr [3]. Nationally and globally, the additional fuel consumed due to air conditioner usage is substantial. A study by Rugh et al. [2] indicate air conditioner usage reduces fuel economy by about 20% and increases emissions of nitrogen oxides (NO_x) by about 80% and carbon dioxide (CO) by about 70%, although the actual numbers depend on the actual driving conditions.

Due to the ascending trend in the rate emission of pollutant, the automotive industry has been compelled to accomplish parallel development of both environmental awareness and fuel economy by establishing innovative solutions to improve the quality of the urban environment and to reduce the rate of fuel consumption to drive the compressor air conditioner and the climate control system in total. The

solutions include the use of solar reflective glass [2, 4], parking cooling systems for non-idling air-conditioning [5], demand capacity controlled compressor [6], air inlet mixture control strategy [7, 8], automatic climate control systems [9,10] and reduction in weight and size of air conditioning units [11].

The energy crisis can be avoided by using renewable energy or it can be delayed via efficient utilisation of the existing non-renewable energy reserves. The latter approach is probably the only means of avoiding an impending crisis before a practical and economically viable method of harnessing free energy is found since research efforts on renewable energy (such as solar and wind energy) are still on-going. In order to accomplish this goal, an efficient and comprehensive tool for rapid design and prototyping of AAC system for analysis is needed. It also must be noted that, increasing the activities of experimentation and prototyping of any air-conditioning system, may increase the cost and price tag, especially for automotive manufacturers of developing countries. In this respect, computer simulation can be used for rigorous analysis of the cabin thermal load and air conditioner interaction. Simulation is economical and not harmful to the environment, unlike actual testing of prototypes.

Several integrated models for analyzing AAC performance have appeared in the open literature [2, 12, 13, 14, 15, 16, & 17]. Most of them used computational fluid dynamic (CFD) and lumped-parameter approaches. Generally, the CFD scheme is restricted to steady-state cases or very short simulation periods [18] whereas lumped parameter approach involves more analytical efforts and computer time than those dedicated by the original problem [19]. As a result, in this study, a unique approach is adopted in developing a computerised simulation tool for analysing the thermal and energy performance of the AAC system in passenger vehicles. The cabin compartment dynamic loads simulation is made on a minute-by-minute basis using the z-transfer function methodology. The methodology has been widely used by building energy simulation programs on an hour-by-hour time interval, but it is rarely been used in load simulation of passenger vehicles. By using one-minute time interval, it is possible to capture the dynamics of energy transfer and storage of the vehicles more accurately. The newly developed tool also directly considers the performance of the evaporator coil by linking the thermal loads model and actual coil sensible and latent heat transfer performance. As a result, this semi-empirical simulation tool is not only comprehensive but also capable of modelling realistically the actual processes that occur in actual vehicles.

2. Dynamic Loads Analysis Of Passenger Cabin

According to ASHRAE [20] load analysis methods in an enclosed space can be classified into two groups: steady-state methods and dynamic methods. Dynamic methods are more attractive than the steady-state method as they are able to model complex phenomena as well as being more flexible. The two widely used dynamic methods are the heat balance method (HBM) and the weighting factor method (WFM) [20]. The HBM is more accurate than WFM. The simple WFM is chosen over the more rigorous HBM for loads calculation in a passenger vehicle for ease of simulation with some small loss in accuracy which explains why most of the popular building energy simulation programs adopt the weighing factor methodology.

2.1 The Weighting Factor Method

The WFM is able to accelerate loads calculation by using a simplified procedure [21]. It uses heat gain weighting factors for converting heat gains to cooling loads, followed by the use of another set of weighting factors to determine heat extraction rates and space air temperatures. Heat gain weighting factors represent parameters in z-transfer functions that relate space cooling loads to instantaneous heat gains. In contrast, air temperature weighting factors represent parameters in a z-transfer function that relates space air temperature to the net sensible heat removal rate.

The heat gain weighting factors are determined by solving the heat balance equations for the space when a unit triangular pulse of space radiant heat gain is applied to the space. The calculation of these factors is subjected to some initial and boundary conditions. At each time step, including the time of introduction, the calculated heat flow to the space air represents the net cooling load which is also the heat gain weighting factor. The cooling load for each type of heat gain is calculated, from [20],

$$Q_k = v_0 q_k + v_1 q_{k-1} + \ldots - w_1 Q_{k-1} - w_2 Q_{k-2} \ldots \qquad (1)$$

where Q_k is the actual cooling load at time k, q_k is the actual heat gain at time k, and $v_0, v_1 \ldots w_1, w_2, \ldots$ are the weighting factors.

The air temperature weighting factors can be determined by solving the heat balance equations for the space when a unit triangular pulse in space air temperature is introduced to the space to generate a sequence of net heat extraction rates. The weighting factors are then calculated using z-transfer function, which relates the net heat extraction rate and the deviation in room air temperature from a constant

value [21]. The deviation of the air temperature from the reference value at time *k*, tr_k is calculated as follows [20],

$$tr_k = \frac{1}{g_0}\left[\begin{array}{l}(CL_k - ER_k) + p_1(CL_{k-1} - ER_{k-1}) + \\ p_2(CL_{k-2} - ER_{k-2}) + ... - g_1 T_{k-1} - g_2 T_{k-2} - ...\end{array}\right] \quad (2)$$

where CL_k is the total cooling load at time *k*, ER_k is the heat extraction rate of the air-conditioning system at time *k*, and $(g_0, g_1, ..., p_1, p_2)$ are the air temperature weighting factors. These factors contain information about the space, particularly the thermal storage capacity of the enclosing elements. Figure 1 shows the overview of the WFM in calculating the space air dry-bulb temperature and heat extraction rate.

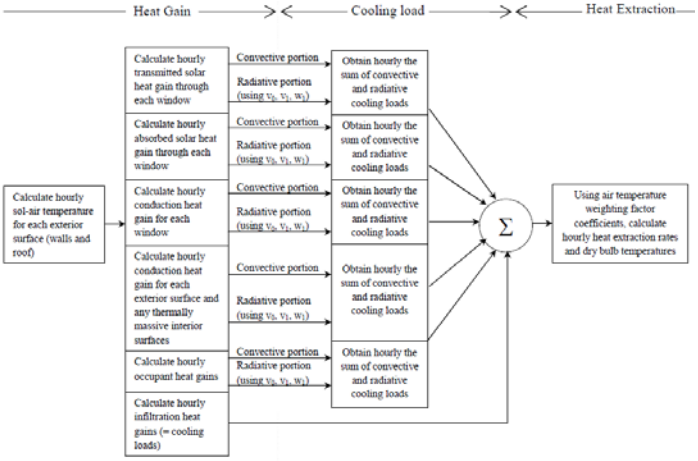

Figure 1 Overview of the WFM in calculating the space air dry-bulb temperature and heat extraction rate [29].

2.2 Thermal Response Factors

The application of weighting factor method requires the determination of heat gain weighting factors (v_0, v_1,) and air temperatures weighting factors (g_0, g_1, g_2,…). In the heat balance equations to obtain these factors, transient heat conduction in solid materials is most easily calculated using thermal response factors (TRFs). TRFs are the heat fluxes at the inside and the outside surfaces of a plane slab [22] as shown in Figure 2. These heat fluxes result from a unit triangular surface temperature pulse excitation. Transient one-dimensional heat conduction problems can be easily solved using the thermal response factor method [20]. The major difficulty is in determining the TRFs.

Specifically, the *Z* and *Y* factors are the heat fluxes in to the inside surface and out of the outside surface of a slab, respectively, when a unit triangular temperature pulse is applied at the inside surface. When the pulse is applied at the outside surface, the *X* and *Y* factors represent heat fluxes in to the outside surface and out of the inside surface, respectively. Generally, car envelopes such as walls, floor and roof are essentially composite layers of materials with different thermo-physical properties. For these multi-layer elements, TRFs are obtained using the explicit finite-difference method for solving the transient one-dimensional Fourier heat conduction equation [23].

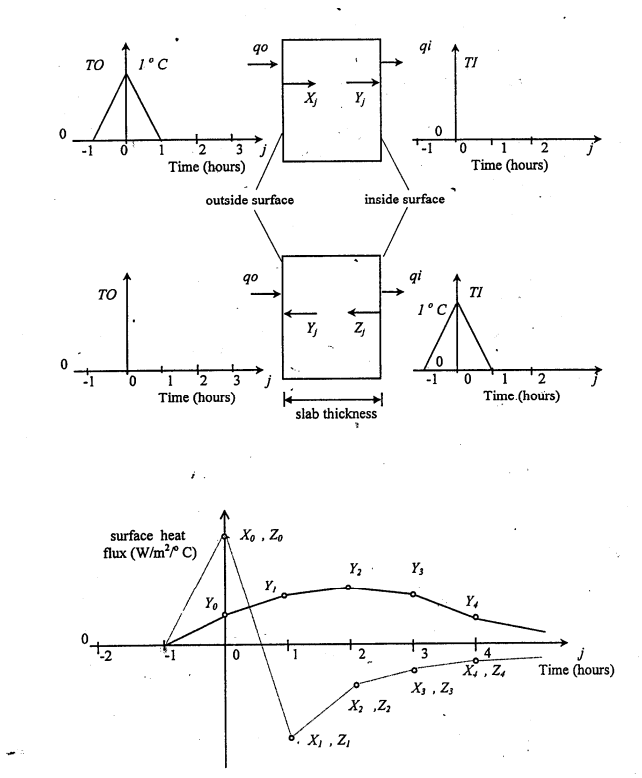

Figure 2 Schematic representation of thermal response factors [30].

2.3 Hourly Heat Gains

Hourly heat gain due to conduction through opaque materials is computed using the transmission matrix method described by Buffington [24] as follows,

$$\begin{bmatrix} t_0 \\ q_0 \end{bmatrix} = \begin{bmatrix} A & B \\ C & D \end{bmatrix} \begin{bmatrix} t_i \\ q_i \end{bmatrix} \quad (3)$$

where,

t_i = inside surface temperature of the layer, °C.

t_0 = outside surface temperature of the layer, °C.

q_i = inside surface heat flux, W/m^2

q_0 = outside surface heat flux, W/m^2

This approach assumes that the outdoor air temperature and solar radiation intensity vary in a periodic manner. Periodic

boundary condition is applied at the outer surface to obtain the analytical solution in terms of a Fourier series consisting of various harmonics. When allowing for a combined radiative-convective inside and outside surface air film resistances, extra layers of a wall or roof are included in the calculation [25]. Thus, for a wall or a roof, t_0 represents the sol-air temperature as given by ASHRAE [20], whereas t_i represents the cabin air dry-bulb temperature.

Solar radiation heat gain through glass windows consists of transmitted, reflected and absorbed components. The internal heat gain due to occupants consists of both sensible and latent heat components. Both heat gains are computed using the method of ASHRAE [20].

3. Experimental Work

Complete simulation of the thermal performance of air-conditioning system for a passenger car requires evaporator coil performance data. This can be obtained either by simulation, as shown by Huang [14] or from experimental data. The former gives approximate solution while the latter will give actual performance data of the evaporator coil. The latter approach was adopted in this work to acquire a realistic model for simulating the thermal and energy performance of an automotive air-conditioning system in the passenger car. Experimental work was conducted to generate the air-side performance data of the evaporator coil for the air conditioner of a 1.6L Proton Wira Aeroback saloon car model.

3.1 Experimental Setup

The experimental setup consisted of three sections: (1) AAC circuit, (2) a closed air duct work for the evaporator section, and (3) an open air duct work for condenser section as shown in Figure 3.

The AAC was a thermal expansion valve system type. The ductworks were designed and constructed in accordance to the British Standard (BS 5141: Part 1: 1975) for of duct-mounted air cooling coils. The AAC system consists of the original components of Denso air conditioning system used in a compact size passenger vehicle (1.6L Proton Wira Aeroback) using HFC134a as the refrigerant. The main components of the AAC system included a swash-plate compressor, an evaporator, a condenser, an expansion valve, a receiver drier, a sight glass and connection pipes.

The air duct work for the evaporator section is a closed loop rectangular circuit with an overall length of 5130 mm. The duct walls between the downstream and upstream of the evaporator coil were thermally insulated using 25 mm thick rock wool insulation material. Air was forced through the evaporator coil using an upstream variable speed

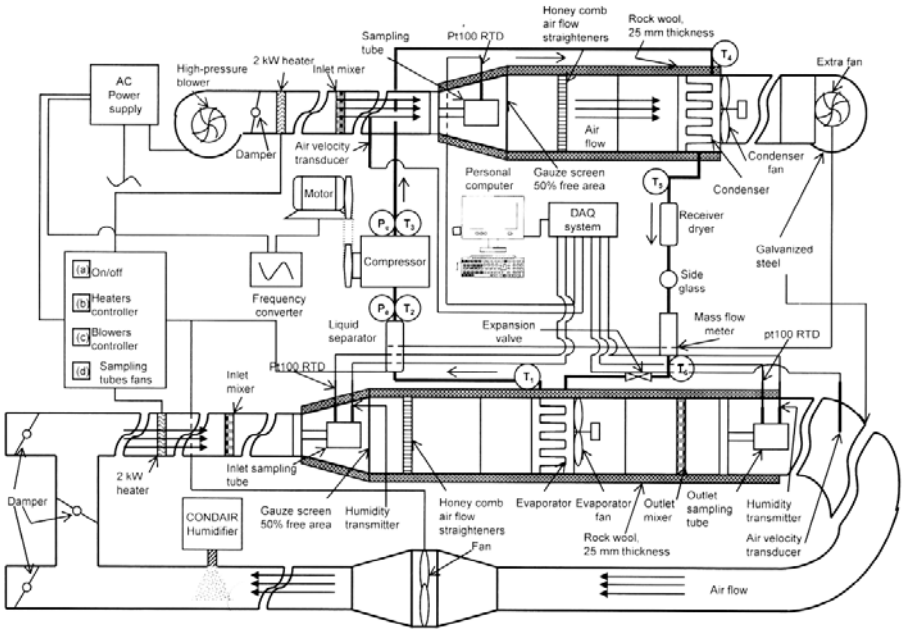

Figure 3 Schematic diagram of the automotive air-conditioning (AAC) system.

centrifugal fan. To improve the air quality, air mixer, honey comb air flow straightener and gauze screens were installed upstream of the evaporator coil. The internal loads were simulated using a 2 kW infra red electrical heaters. A steam humidifier with the steam output of 4 kg/h was incorporated in the ducting system to inject water vapor into the air stream to provide humidity variation. The heating and humidification sections were used to adjust the air temperature and humidity at the evaporator coil entrance.

The air duct work for the condenser section was a rectangular open tunnel with an overall length of 663 mm. Air was forced through the condenser coil using an upstream constant speed high pressure blower (10 HP). To provide variation of face air velocity at the condenser, the blower speed was controlled by using a reducer unit and damper. To improve the air quality in the duct work, similar arrangements as described for the evaporator were employed. A 2 kW infra red air heater was used to vary the air dry bulb temperature at the inlet of the condenser coil.

3.2 Measuring Instruments

The air section of the air-conditioning system was fully instrumented to record and control the operating parameters. The data acquisition system consisted of a standard laptop computer with PCMCIA slot, a data acquisition PCMCIA card and signal conditioning rack. The interface card used was a NI- PCMCIA-6024E multifunction DAQ card featuring 16 analogue inputs at 200 kS/s, 12 bits resolution, 2 analogue outputs, 8 digital I/O lines and digital triggering. The card was interfaced to the laptop computer running DEWESOFT software. The signal conditioning rack was a Dewe-Rack-8 type, with 8 slot mainframe for DEWETRON modules, connection cables for 8 channels rack to NI- PCMCIA-6024E DAQ card, cables for RS-232 and RS-485 interface, and DAQP and PAD modules.

All DAQP and PAD modules were communicating with DEWETRON system through RS-485 and RS-232 interfaces. The DAQP modules were used for velocity and humidity measurement with an accuracy of ±0.05%. The PAD modules were used for RTD temperature sensors with ±0.1% accuracy. In this system, only seven modules were actively used, specifically, two DAQP modules for velocity measurement, two DAQP modules for humidity measurement and three PAD modules for RTD temperature sensors.

Two RTD temperature sensors were used to measure the Two air velocity windowless transducers with an accuracy of ±0.5% and probe length of 6 inches were used to measure the air velocity distribution across the evaporator ductwork cross section and the condenser ductwork cross section. To obtain average air velocity in the ducts, a series of velocity readings have been taken using a single air velocity transducer placed successively at each measuring point as shown in Figure 4 for evaporator ductwork and Figure 5 for condenser ductwork. air dry bulb temperature distribution across the cross section just upstream and down-stream of the evaporator coil.

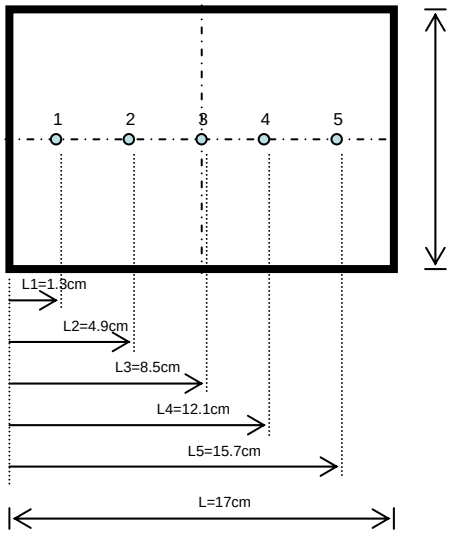

Figure 4 Position of the measuring points in the evaporator ductwork.

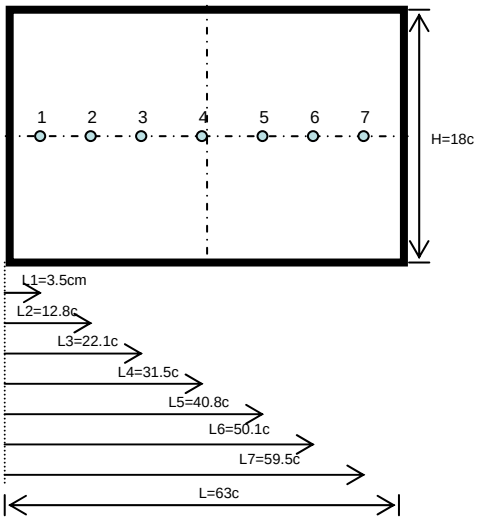

Figure 5 Position of the measuring points in the condenser ductwork.

Another RTD temperature sensor was used to measure the air dry bulb temperature distribution across the condenser cross section downstream of the condenser coil. All temperature sensors were pt100 RTD 100 ohm model made of stainless steel with a length and diameter of 6 inches and 6 mm, respectively. All temperature sensors were connected to PVC air sampling tubes as recommended by BS 5141: Part 1:1975 [20]. The RTD temperature sensors has an accuracy of ±0.3^{o}C has been calibrated by the

manufacturer and has been verified using standard thermometer having an accuracy of ±0.2°C.

Two air velocity windowless transducers with an accuracy of ±0.5% and probe length of 6 inches were used to measure the air velocity distribution across the evaporator ductwork cross section and the condenser ductwork cross section. To obtain average air velocity in the ducts, a series of velocity readings have been taken using a single air velocity transducer placed successively at each measuring point as shown in Figure 4 for evaporator ductwork and Figure 5 for condenser ductwork.

Point sampling for each set of experimental work is time consuming. To overcome this problem a correlation is obtained between averaged air velocity and the centre point air velocity. Least squares regression yields the correlations for evaporator ductwork with a coefficient of determination, $r^2 = 0.997$ and for condenser ductwork with $r^2 = 0.977$. The subsequent experiments were conducted by taking one reading at the centre of the ductwork only and the average air velocities are obtained from the correlations. Two Honeywell humidity sensors model 4129R with measuring range of 0 to 100% RH with an output of 4-20mA and accuracy of ±1% were used to measure the air relative humidity just upstream and downstream of the evaporator coils.

3.3 Description of the Test Procedures

The experimental work was conducted at steady-state conditions. The tests were run at different compressor speeds with varying heat load at the coil. The compressor speed was set at 1500, 2000, 2500 and 3000 rpm by controlling the motor speed using a frequency inverter. At each compressor speed, the air flowing through the condenser was adjusted between 2.2 and 4.8 m/s using a reducer unit and damper. At each air velocity through the condenser, the air velocity of the evaporator coil was maintained at blower speed 1, blower speed 2, blower speed 3 and blower speed 4. At each blower speed, the air dry-bulb temperature at the inlet of the evaporator was kept at 25, 30 and 35°C by varying the energy input to the electric heater upstream of the evaporator. At each evaporator inlet air temperature, the air dry-bulb temperature at the inlet of the condenser was set at 32, 35 and 40°C, by varying the energy input to the electric heater upstream of the condenser. To stabilize the air-conditioning system, the air conditioner was run 30 minutes prior to each test. Table 1 shows the ranges of the test variables applied in the study.

Table 1 The ranges of the test variables applied in the study.

Test variable	Ranges
Compressor speed, N_c	1500 - 3000 rpm
Air velocity through the condenser, V_c	2.2 - 4.8 m/s
Air velocity through the evaporator, V_e	2.5 - 5.5 m/s
Evaporator inlet air dry-bulb temperature, t_{ei}	25 - 30°C
Condenser inlet air dry-bulb temperature, t_{ci}	32 - 40°C

3.4 Development of Empirical Correlations

A multi-linear regression of the 273 experimental data has been made to fit two power equations. These power equations were obtained using the standard regression method described by Chapra and Canale [26]. The independent variables are the compressor speed, N_c (rpm), the coil (evaporator) inlet air dry-bulb temperature, t_1 (°C), the coil air face velocity, V_e (m/s), the condenser air face velocity, V_c (m/s), the condenser inlet air dry bulb temperature, t_{ci} (°C), and the coil inlet air specific humidity, w_1 (kg_v/kg_{da}).

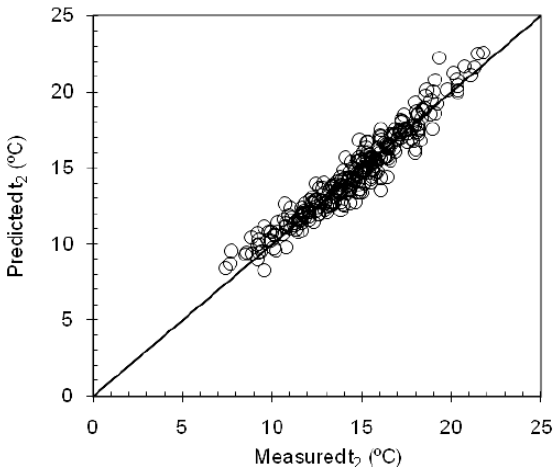

Figure 6 Predicted and measured coil air off dry-bulb temperatures.

The first correlation relates the coil air off dry bulb temperature, t_2 (°C) to the independent variables,

$$t_2 = 2.67104(N_c)^{-0.2155}(t_{e_i})^{0.4472}(V_e)^{0.4319}(V_c)^{-0.0882} \ldots(t_{c_i})^{0.4799}(w_1)^{0.4623} \quad (4)$$

The second correlation relates the coil air off specific humidity, w_2 (kg/kg) to the independent variables and as follows,

$$w_2 = 0.00206(N_c)^{-0.1590}(t_{e_i})^{0.4289}(V_e)^{0.5103}\ldots$$
$$(V_c)^{-0.0977}(t_{c_i})^{0.4438}(w_1)^{0.4784} \quad (5)$$

Figure 6 shows the predicted coil air off dry bulb temperature of equation (4) compared to the measured values. The degree of agreement is very good with the coefficient of determination, r^2 of 0.94. A plot of predicted coil air off specific humidity of equation (5) against measured data also indicates good agreement with $r^2 = 0.92$, as shown in Figure 7.

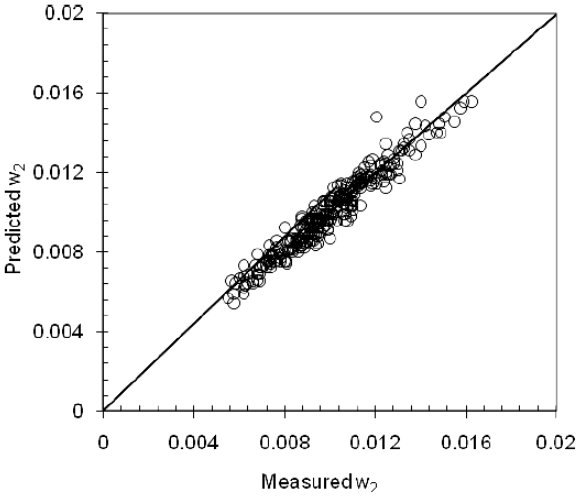

Figure 7 Predicted and measured coil air off specific humidity.

4. Car Simulation (CARSIM) Program

Figure 8 shows the flow chart for the program. The input data are submitted in three files, each with different types of data. The first file contains the thermo-physical data of the car, the second file contains the custom z-transfer function weighting factors for the car, and the last file contains the twenty-four hourly weather data.

A separate system program named **WFAC** was used to specifically generate two sets of weighting factors: heat gain weighting factors (v_0, v_1, …) and air temperature weighting factors (g_0, g_1, ..) that are required by the CARSIM program. The weighting factors were calculated for a one minute simulation time interval.

The weather data submitted to CARSIM consisted of typical days of actual weather data for a twenty-four hour period. The outdoor air data are the dry bulb temperature, specific humidity, and direct and diffuse solar radiation intensity on the horizontal plane. Transient heat conduction through roof, walls and floor are calculated using the transmission matrix method.

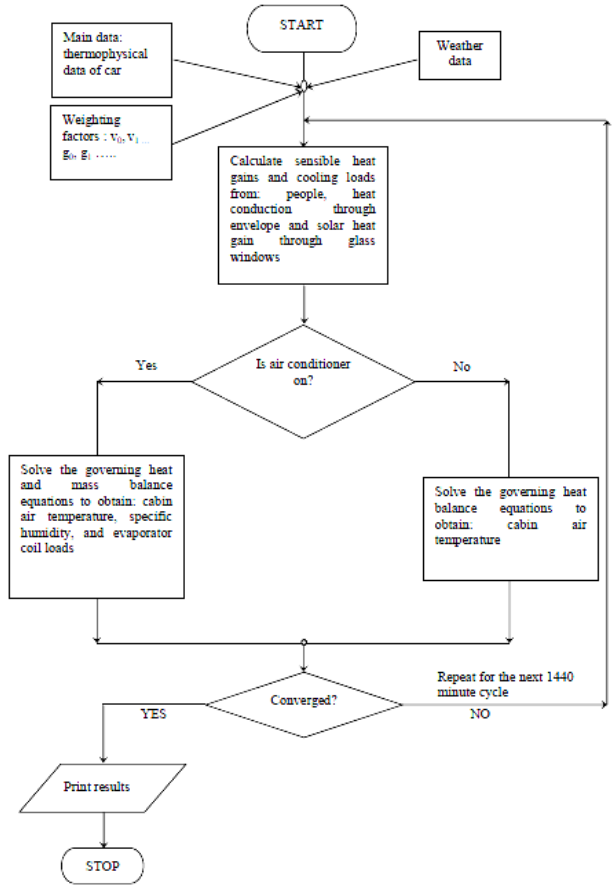

Figure 8 Flow chart for the CARSIM program.

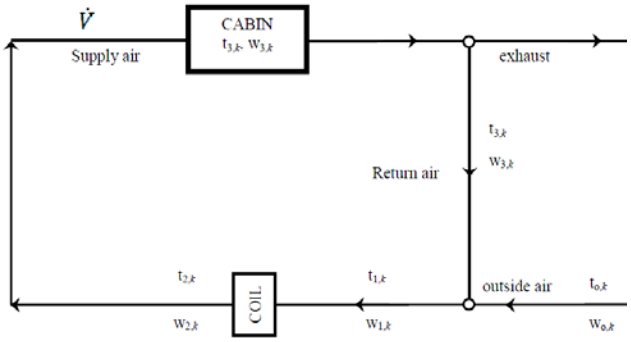

Figure 9 Simplified schematic diagram of car air conditioning system.

Heat gain weighting factors are then used to convert the heat gains to cooling loads using the heat gain weighting factors. Solar heat gains are calculated using the method described by ASHRAE [19], followed by conversion to cooling loads using the weighting factors obtained from WFAC. The total cooling load profile is then used to calculate the cabin air dry bulb temperature and specific humidity when the air conditioner is functioning. When the air conditioner is not active, only cabin air dry bulb temperature is calculated.

Figure 9 shows the simplified schematic diagram of the air conditioning system of a passenger vehicle. During the period the air conditioner is active, the seven governing equations with seven unknowns are [27]:

$$ER_k - CL_k = \sum_{j=0}^{\infty} g_j (TRC - t_{3,k-j}) \quad \text{W} \tag{6}$$

$$ER_k = 1.23V(t_{3,k} - t_{2,k}) \quad \text{W} \tag{7}$$

$$t_{2,k} = a_0 N_c^{a1} t_{1,k}^{a2} V_e^{a3} V_c^{a4} t_{0,k}^{a5} w_{1,k}^{a6} \quad {}^{o}C \tag{8}$$

$$w_{2,k} = b_0 N_c^{b1} t_{1,k}^{b2} V_e^{b3} V_c^{b4} t_{0,k}^{b5} w_{1,k}^{b6} \quad \text{kg/kg} \tag{9}$$

$$Q_{L,k} = 3010\dot{V}(w_{3,k} - w_{2,k}) \quad \text{W} \tag{10}$$

$$t_{1,k} = (XOA)t_{0,k} + (1 - XOA)t_{3,k} \quad {}^{o}C \tag{11}$$

$$w_{1,k} = (XOA)w_{0,k} + (1 - XOA)w_{3,k} \quad \text{kg/kg} \tag{12}$$

where,

$t_{0,k}$ = ambient air dry bulb temperature at time *k*, °C

$t_{1,k}$ = coil inlet air dry bulb temperature at time *k*, °C

$t_{2,k}$ = coil outlet air dry bulb temperature at time *k*, °C

$t_{3,k}$ = cabin air dry bulb temperature at time *k*, °C

$w_{0,k}$ = ambient air specific humidity at time *k*, kg/kg

$w_{1,k}$ = coil inlet air specific humidity at time *k*, kg/kg

$w_{2,k}$ = coil outlet air specific humidity at time *k*, kg/kg

$w_{3,k}$ = cabin air specific humidity at time *k*, kg/kg

ER_k = heat extraction rate of cabin at time *k*, W

CL_k = total sensible cooling load of cabin at time *k*, W

$Q_{L,k}$ = cabin latent load (from occupant) at time *k*, W

XOA = fraction of outside air

N_c = compressor speed, rpm/1000

V_e = air velocity at coil outlet, m/s

V_c = condenser air face velocity, m/s

a_0, a_1, a_2, a_3, a_4, a_5, a_6 = coil sensible heat correlation coefficients (see Eq. (4))

b_0, b_1, b_2, b_3, b_4, b_5, b_6 = coil latent heat correlation coefficients (see Eq. (5))

The seven unknowns are $t_{1,k}$, $t_{2,k}$, $t_{3,k}$, $w_{1,k}$, $w_{2,k}$, $w_{3,k}$ and ER_k. Equations (6) through (12) are solved by iteration. When air conditioning is not active, the solution for cabin air temperature is obtained by simply setting ER_k in equation (6) to zero to give

$$t_{3,k} = \frac{CL_k + TRC + \sum_{j=1}^{\infty} g_j (TRC - t_{3,k-j})}{g_0} \tag{13}$$

Constant room temperature (TRC) is the one-day averaged cabin air temperature. Initially, a value is assumed for TRC, and it is updated after each one-day cycle of calculation. Convergence is achieved when

$$\varepsilon = \left| \frac{TRC_{old} - TRC_{new}}{TRC_{old}} \right| \leq 0.001 \tag{14}$$

For a typical simulation, convergence is attained after about five to six cycles of calculation, with 1440 minutes calculation per cycle. With air conditioning turned on, the coil sensible load, $Q_{C,S}$ and the coil latent load, $Q_{C,L}$ are calculated as follows:

$$Q_{C,S} = 1.23\dot{V}(t_{1,k} - t_{2,k}) \quad \text{W} \tag{15}$$

$$Q_{C,L} = 3010\dot{V}(w_{1,k} - w_{2,k}) \quad \text{W} \tag{16}$$

4.1 Validation of CARSIM Program

The test vehicle used was a four-door 1.6L Proton Wira Aeroback. The age of the vehicle was about four years. The vehicle and its air conditioning system have gone through standard maintenance routines, and were in good operating condition.

4.1.2 Test Setup

The experimental road test was carried out from October to November 2008. During each test, there were two to three occupants in the vehicle cabin, including the driver. Each trip began in Skudai, Johor on city streets, progressed north on PLUS highway to Pagoh, Johor, regressed to south on the same highway and ended in Skudai, Johor. Total mileage for each test was approximately 300 kilometres.

The objective of the test was to measure the cabin air dry-bulb temperature of the test vehicle. The tests were performed at two different vehicle speeds, 90 km/h and 105 km/h respectively. These speeds were chosen so that the compressor speeds of the air conditioning system were similar to the speeds during the laboratory test. For each vehicle speed, the air blower was regulated at blower speed 1 and blower speed 4. For each condition, the temperature was recorded at every two to five minutes for 10 to 20 minutes duration depending on the weather and traffic condition during the test.

A total of eight type-*T* thermocouples were used to measure cabin temperature distribution as shown in Figure 10. All thermocouples were connected to a data acquisition system through extension wire to record thermocouples readings as shown in Figure 11.

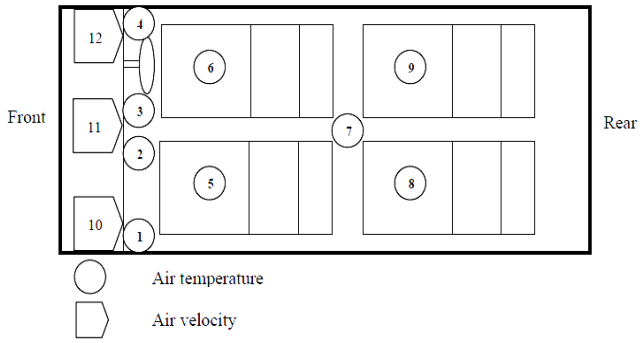

Figure 10 Locations for data measurement (top view).

The data acquisition system consisted of a standard notebook with USB TC-08 furnished with a PicoLog software. The thermocouples were calibrated using standard thermometer of accuracy $\pm 0.2^{o}C$. The cabin supply airflow velocity was measured at frontage of the air vents by using a Testo 450 vane anemometer. The vane anemometer measuring ranges were between 4 to 40 m/s, with an accuracy of 0.5%. These test data were used as a basis for comparison with the predictions by CARSIM program, for the same vehicle type.

Figure 11 Experiment apparatus: (A) USB TC-08 is connected to a laptop; (B) Temperature reading displayed on line; (C) USB TC-08; (D) Thermocouples arrangement.

4.2 Comparison Between Simulation and Test Data

The CARSIM program requires thermo-physical data of the test car as input data. Figure 12 shows a typical simplified model of the test car. The air-conditioned floor area and passenger cabin volume were 2.33 m^2 and 2.54 m^3, respectively. For zoning purposes, it was modelled as one thermal zone.

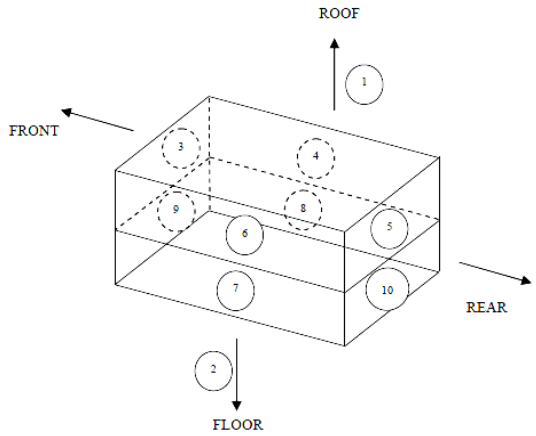

1 - Roof
2 - Floor
3 - Front window
4. 6 - Side windows
5 - Rear window
7. 8 - Side walls
9 - Metal panel
10 - Rear seat and metal panel

Figure 12 Typical simplified model of the test car.

The CARSIM program used the typical weather data for Singapore for the November– December months. The weather data was a ten-year averaged actual weather data developed by Moller and Wooldridge [28] for the computer program BUNYIP.

The CARSIM program predictions of the air dry-bulb temperature variation inside the car cabin are shown in Figures 13 through 16. Figure 13 shows the averaged air dry-bulb temperature variation for the vehicle speed of 105 km/h, air-conditioning (A/C) fan blower at level 4 and three occupants.

Figure 14 shows the averaged air dry-bulb temperature variation for the vehicle speed of 105 km/h, A/C fan blower at level 1 and three occupants. Figure 15 shows the averaged air dry-bulb temperature variation for the vehicle speed of 90 km/h, A/C fan blower at level 4 and three occupants. Finally, Figure 16 shows the averaged air dry-bulb temperature variation for the vehicle speed of 90 km/h, A/C fan blower at level 1 with three occupants.

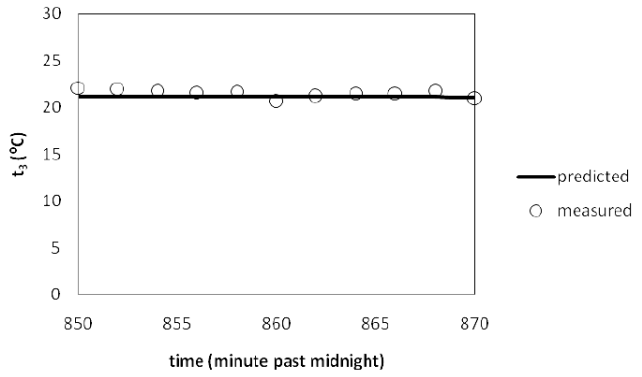

Figure 13 Variation of car cabin air temperature for vehicle speed of 105 km/h, blower 4 and three occupants.

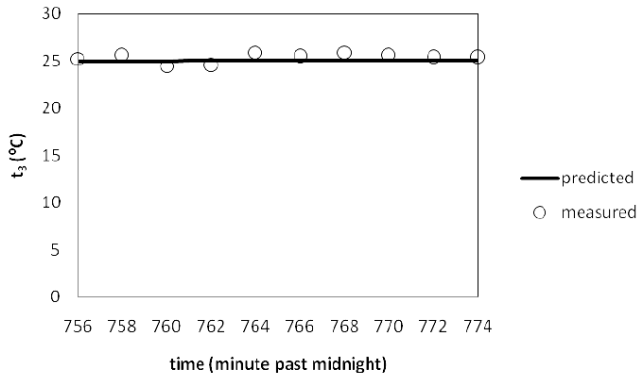

Figure 14 Variation of car cabin air temperature, t_3 for vehicle speed of 105 km/h, blower 1 and three occupants.

As seen from Figure 13, the predicted temperatures are in a good agreement with the test data with a deviation of 0.5ºC in average. Overall, the CARSIM program estimates of zone temperature are slightly lower than those obtained from the test data. The predicted data is about 0.25% to 4.05% lower than the experimental data. Figure 14 shows that the deviations between predicted and measured values are between 0.86% and 3.32%. Figure 15 shows that the agreement between predicted and measured temperatures is quite good, with a deviation of 0.57ºC on average. The largest and lowest deviations are 4% and 0.31% respectively. Overall, the predicted values of zone temperature are slightly higher than those obtained from the test data.

Figure 16 shows that the agreement between the predicted and measured temperatures is quite good, with a deviation of 0.29ºC on average with maximum and minimum errors of about 2.69% and 0.2% respectively. It is evident that the agreement between predicted and measured car cabin temperatures is good.

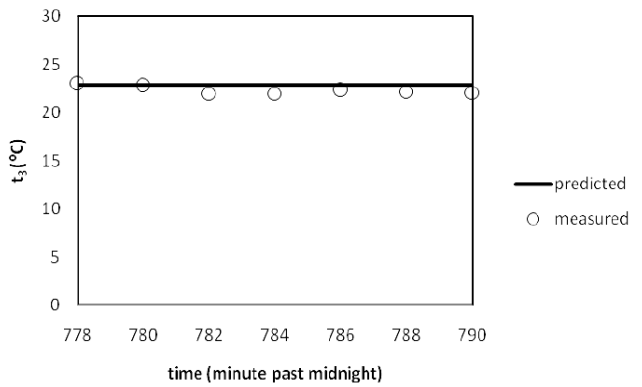

Figure 15 Variation of car cabin air temperature, t_3 for vehicle speed of 90 km/h, blower 4 and three occupants.

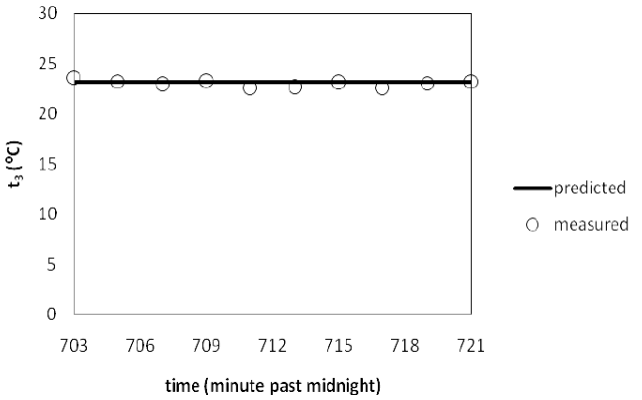

Figure 16 Variation of car cabin air temperature, t_3 for vehicle speed of 90 km/h, blower 1 and two occupants.

5. Conclusion

A semi-empirical computerized simulation program (CARSIM) for simulating the thermal and energy performance of an automotive air-conditioning system has been developed based on the z-transfer function method. The empirical evaporator sensible and latent heat transfer correlations embedded in the loads calculation program enable the determination of evaporator inlet and outlet air conditions and the cabin air conditions. The program was validated using data obtained from actual road test for various operating conditions. The results obtained from the CARSIM program were found to agree very well with those obtained from actual road test, with a discrepancy of 2 to 4%.

Acknowledgement

The authors would like to acknowledge the support from Universiti Teknologi Malaysia and funding provided by Ministry of Science, Technology and Innovation, Malaysia

and Research Management Centre, Universiti Teknologi Malaysia through IRPA grant 74062.

References

[1] Amr Gado, Yunho Hwang and Reinhard Radermacher, Dynamic Behavior of Mobile Air-Conditioning Systems. ProQuest Science Journals; HVAC&R Research 14 (2) (2008) 307 – 312.

[2] Rugh, J. P. and Hendricks, T. J., Effect of Solar Reflective Glazing on Ford Explorer Climate Control, Fuel Economy, and Emissions. Society of Automotive Engineers (SAE) Technical Paper Series. Paper No. 2001-01-3077.

[3] Johnson, H. V., Fuel Used for Vehicle Air Conditioning: A State-by-State Thermal Comfort-Based Approach. Society of Automotive Engineers (SAE) Technical Paper Series. Paper No. 2002-01-1957.

[4] Farrington, R. B., Rugh, J. P. and Barber, G. D., Effect of Solar Reflective Glazing On Fuel Economy, Tailpipe Emissions and Thermal Comfort. Society of Automotive Engineers (SAE) Technical Paper Series. Paper No. 2000-01-2694.

[5] Kampf, H. and Schmadl, D., Parking Cooling Systems for Truck Cabins. Society of Automotive Engineers (SAE) Technical Paper Series. Paper No. 2001-01-1728.

[6] Watanabe, Y. and Sekita, M., Saving Power by Demand Capacity Controlled Compressor. Society of Automotive Engineers (SAE) Technical Paper Series. Paper No. 2002-01-0232.

[7] Forrest, W. O. and Bhatti, M. S., Energy Efficient Automotive Air Conditioning System. Society of Automotive Engineers (SAE) Technical Paper Series. Paper No. 2002-01-0229.

[8] M. Khamis Mansour, Md Nor Musa, Mat Nawi Wan Hassan and Khalid M. Saqr, Development of Novel Control Strategy for Multiple Circuit, Roof Top Bus Air Conditioning System in Hot Humid Country. Energy Conversion and Management. 44 (2008) 1455–1468.

[9] Michalek, D., Gehsat, C., Trapp, R. and Bertram, T., Hardware-in-the-loop-Simulation of a Vehicle Climate Controller with a Combined HVAC and Passenger Compartment Model. Advanced Intelligent Mechatronics; Proceedings, 2005 IEEE/ASME International Conference on Digital Object Identifier. (2005) 1065-1070.

[10] Farzaneh, Y. and Tootoonchi, A. A., Controlling Automobile Thermal Comfort Using Optimized Fuzzy Controller. Applied Thermal Engineering. 28 (2008) 1906–1917

[11] Jin, J., Chen, J. and Chen, Z., Development and Validation of a Microchannel Evaporator Model for a CO2 Air-conditioning System. Applied Thermal Engineering. Development of Compact Heat Exchangers for CO2 Air-conditioning Systems. Applied Thermal Engineering (2010), doi: 10.1016/ j.applthermaleng.2010.06.019.

[12] Kohler, J., Kuhn, B. and Beer, H., Numerical Calculation of The Distribution of Temperature And Heat Flux In Buses Under The Influence of The Vehicle Air-Conditioning System. ASHRAE Transactions. 96 (Part 1) (1990) 432 – 446.

[13] Currle, J., Harper, M., Ross and F., Heid, T., Evaluation of HVAC System of Passenger Cars and Prediction of The Microclimate in The Passenger Compartment by Application of Numerical Flow Analysis. Society of Automotive Engineers (SAE) Technical Paper Series. (1997) Paper No. 971788.

[14] Huang Chi-Chang Daniel, A Dynamic Computer Simulation Model For Automobile Passenger Compartment Climate Control and Evaluation. PhD Thesis Michigan Technological University (1998).

[15] Khamsi, Y. and Petitjean, C., Dynamic Simulation of Automotive Passenger Compartment And It's Air Conditioning System. Society of Automotive Engineers (SAE) Technical Paper Series. Paper No. 2000-01-0982.

[16] Ali Heydari and Saeed Jani, Entropy-Minimized Optimization of an Automotive Air-conditioning and HVAC System. Society of Automotive Engineers (SAE) Technical Paper Series. Paper No. 2001-01-0592.

[17] Rugh, J., Integrated Numerical Modeling Process for Evaluating Automobile Climate Control Systems. Society of Automotive Engineers (SAE) Technical Paper Series. (2002) Paper No. 02FCC-70.

[18] Hensen, J., Bartak, M. and Drkal, F., Modeling and Simulation of a Double-Skin Facade System. ASHRAE Transactions. 108 (2) (2002) 1251-1259.

[19] Ingersoll, J. G., Thomas, G. K., Maxwell, L. M. and Niemec, R. J., Automobile Passenger Compartment Thermal Comfort Model – Part 1: Compartment Cool-Down / Warm-Up Calculation. Society of Automotive Engineers (SAE) Technical Paper Series. Paper No. 920265 232 – 242.

[20] ASHRAE 1993. Handbook of Fundamentals. Atlanta, GA: American Society of Heating, Refrigerating and Air-Conditioning Engineers, Inc.

[21] Mitalas, G. P., Comments on the Z-Transfer Function Method for Calculating Heat Transfer in Building. ASHRAE Transactions. 84 (1) (1978) 667-674.

[22] Mitalas, G. P. ,Calculation of Transient Heat Flow Through Walls and Roofs. ASHRAE Transactions. 72 (2) (1968) 182 – 188.

[23] Mohd Yusoff Senawi, Development of A Building Energy Analysis Package (BEAP) And Its Application To The Analysis of Cool Thermal Energy Storage Systems. Ph.D Thesis, University Technology of Malaysia (2000).
[24] Buffington, D. E., Heat Gain by conduction Through Exterior Walls and Roofs – Transmission Matrix Method. ASHRAE Transactions. 81 (2) (1975) 89 – 101.
[25] Mohd Yusoff Senawi, Software Development For Building Energy Analysis. Master Thesis, University Technology of Malaysia (1992).
[26] Chapra, S.C. and Canale, R.P., Numerical Methods for Engineers, Mc Graw Hill, New York, USA 2006.
[27] Haslinda Mohamed Kamar, Computerised Simulation of Automotive Air Conditioning System. Ph.D Thesis, University Technology of Malaysia (2009).
[28] Moller, S. K. and Wooldridge, M. J., User's Guide for the Computer Program BUNYIP: Building Energy Investigation Package (Version 2.0), Highett, Victoria, Australia 1985.
[29] McQuiston, F. C. and Parker, J. D. (1994). Heating, Ventilating, and Air Conditioning Analysis and Design. 4th ed. United States : John Wiley & Sons, Inc.
[30] Kimura, K., Scientific Basis of Air Conditioning. London, Applied Science Publishers Ltd. (1977).

Haslinda Mohamed Kamar, is a member of ASHRAE. She received her Bachelor's Degree in Mechanical Engineering from University of Glasgow, Scotland in 1993, Master and PhD in Mechanical Engineering from University Teknologi Malaysia in 1997 and 2009, respectively. She is now a senior lecturer in the Faculty of Mechanical Engineering, Universiti Teknologi Malaysia. Her areas of interest are automotive air-conditioning system, thermal comfort & energy efficiency in hot climates, indoor air quality (IAQ), natural ventilation as passive cooling strategy in buildings and computational fluid dynamics (CFD) modeling and simulation.

Mohd Yusoff Senawi, graduated with Bachelor of Mechanical Engineering from The University of New South Wales in 1987. Received Post Graduate Diploma in Computer Science, Master and PhD in Mechanical Engineering from Universiti Teknologi Malaysia (UTM) in 1989, 1993 and 2000, respectively. Currently a Senior Lecturer at UTM. Research interests include cooling loads calculation and energy analysis of air conditioning systems.

Nazri Kamsah is a member of ASHRAE. He received his Bachelor's Degree in Mechanical Engineering from University of Sunderland, United Kingdom in 1983, Masters of Engineering (Mechanical) from Universiti Teknologi Malaysia in 1988, and PhD in Mechanical Engineering from University of New Hampshire, Durham, USA in 2001. He is currently a senior lecturer in the Faculty of Mechanical Engineering, Universiti Teknologi Malaysia. His areas of interest include computational solid mechanics, finite element modeling and simulation, thermal management in microelectronics, thermal comfort and energy efficiency in buildings, natural ventilation as passive cooling strategy for buildings, indoor air quality (IAQ) and computational fluid dynamics (CFD) modeling and simulation.